

Texture Analysis of Cirrhosis Liver using Support Vector Machine

Karan Aggarwal*, Manjit Singh Bhamrah**, Hardeep Singh Ryait***

*(Electronics & Communication Engg. Dept., M.M.Engg. College, Mullana
Email: karan.170987@gmail.com)

** (Electronics & Communication Engg. Dept., UCOE, Punjabi University, Patiala
Email: manjitsingh_manjit@rediffmail.com)

*** (Electronics & Communication Engg. Dept., BBSBEC, Fatehgarh Sahib
Email: hardeepsryait@gmail.com)

ABSTRACT

Diagnostic ultrasound is a useful and noninvasive method in clinical medicine. Although due to its qualitative, subjective and experience-based nature, ultrasound image interpretation can be influenced by image conditions such as scanning frequency and machine settings. In this paper, a method is proposed to extract the cirrhosis and normal liver features using the entropy of texture edge co-occurrence matrix based on ultrasound images, which is not sensitive to changes in emission frequency and gain. Then, support vector machine are employed to test a group of 30 in-vivo liver cirrhosis images from 18 patients, as well as other 30 liver images from 18 normal human volunteers. The results showed that the support vector machine is 94.4% in sensitivity for liver cirrhosis (LC) while neural network provided 92.31 % and the system is considered to be helpful for clinical and educational use.

Key words: Cirrhosis liver, Texture, Co-occurrences matrix, Support vector machine.

I. INTRODUCTION

Cirrhosis is a complication of many liver diseases that is characterized by abnormal structure and function of the liver. The diseases that lead to cirrhosis do so because they injure and kill liver cells and the inflammation and repair that is associated with the dying liver cells causes scar tissue to form. The liver cells that do not die multiply in an attempt to replace the cells that have died. This results in clusters of newly-formed liver cells (regenerative nodules) within the scar tissue. Cirrhosis is considered to be the end stage of chronic hepatopathies which often leads to hepatocellular carcinoma. The diagnosis of the disease is best achieved by looking at the granular structure of the liver parenchyma and the aspects of the liver surface such as its unevenness and its contour as shown in Fig. 1.

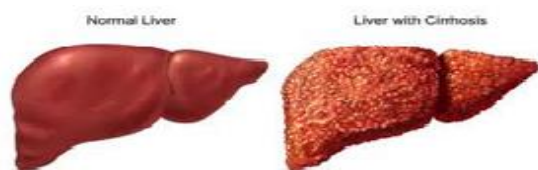


Fig. 1: Granular structure of liver

The discrimination of cirrhosis from its preceding stages of fibrosis is based on visual aspect of the degree of nodularity present in the heterogeneous echo texture, which is often difficult to access visually [1]. Liver biopsy suffers from several important drawbacks like morbidity, observer variability and sampling variation [2]. So, there is a need for developing a noninvasive cirrhosis detection system [4]. In literature, there are a number of papers that propose the texture analysis methods applied on B-mode ultrasound images [3].

For quantitative image analysis many feature parameters have been proposed and used in developing automatic diagnosis system [5][6][7]. The several quantitative features are being used in diagnosis by ultrasonography. A classification method based on artificial neural network to diagnose diffuse liver diseases is developed [8] [10]. In [9] [10][11][12], authors presented the classifier for diagnosis of normal liver (NL), chronic active hepatitis (CAH) and cirrhosis (CRH) more accurately. Quantitative tissue characterization technique (QTCT) is gaining more acceptance and appreciation from the ultrasound diagnosis community. It has the potential to significantly assist radiologists to use this system for second opinion. The grey scale ultrasound images provide significant

contribution to the diagnosis of liver diseases, however at the resolution it is difficult to diagnose active hepatitis and cirrhosis from normal liver [13][14]. A pattern recognition system can be considered in two stages, the first stage is feature extraction and the second is classification [15] [16][17].

In this paper, a method is proposed to extract the liver features using the entropies of texture edge co-occurrence matrix based on ultrasound images, which are not sensitive to changes in emission frequency and gain. Then, support vector machine is applied to a set of cirrhosis images from patients and liver images from normal human volunteers.

II. METHODOLOGY ADOPTED

There are a group of 30 in-vivo liver cirrhosis images from 18 patients, as well as other 30 liver images from 18 normal human volunteers. By using these images, five parameters have been detected and those images are classified through SVM using MATLAB as shown in Fig. 2.

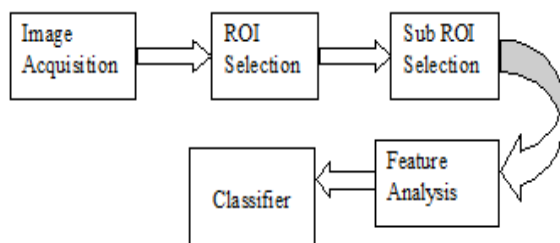


Fig.2: Block Diagram

Parameters are:

A. ENERGY

$$ene = \sum_{i=0}^{N_g-1} \sum_{j=0}^{N_g-1} g^2(i, j)$$

This parameter is also called Angular Second moment [18] and Uniformity in [17] [19] [20]. Energy measures textural uniformity, i.e., pixel pairs repetitions; when the image patch under consideration is homogeneous (only similar gray level pixels are present) or when it is texturally uniform (the vector displacement always falls on the same (i, j) gray level pair), a few (possibly only one) elements of gray level co-occurrence matrix (GLCM) will be greater than 0 and close to 1, while many elements will be close to 0. In this case energy reaches values close to its maximum, equal to 1.

Thus, high energy values occur when the gray level distribution over the window has either a constant or a periodic form [20]. This result means that energy is strongly uncorrelated to first order statistical variables such as contrast and variance. Indeed, energy may reach its maximum either with maximum or no variance and contrast values.

B. ENTROPY

$$ent = - \sum_{i=0}^{N_g-1} \sum_{j=0}^{N_g-1} g(i, j) \cdot \log(g(i, j))$$

This parameter measures the disorder of an image. When the image is not texturally uniform, many GLCM elements have a very small value, which implies that entropy is very large. As an example, consider a window with completely random values of gray level pixel values (white noise). The histogram for such a window is a constant function, i.e., all $g(i, j)$ are the same, and the entropy parameter reaches its maximum [20]. From a conceptual point of view, entropy is strongly, but inversely, correlated to GLCM energy. Theoretically, similar results are expected for energy and entropy clustering. An advantage in using energy rather than entropy lies in the fact that the former has a normalized range.

C. CONTRAST

$$con = \sum_{i=0}^{N_g-1} \sum_{j=0}^{N_g-1} (i - j)^2 \cdot g(i, j) = \overline{\Delta_{con}}$$

Where

$$\Delta_{con} = (i - j)^2$$

Spatial frequency is the difference between the highest and the lowest values of a contiguous set of pixels. This definition holds for the GLCM contrast expression as well, in particular when the module of the displacement vector is equal to one. This implies that a low contrast image is not necessarily characterized by a narrow gray level distribution, i.e., it does not necessarily present a low variance value, but the low contrast image certainly features low spatial frequencies. The conclusion is that the GLCM contrast tends to be highly correlated with spatial frequencies while the module of the displacement vector tends to one. With regard to the GLCM variance and contrast pair, the only condition that relates these two parameters to each other is the following: a sufficient, but not necessary, condition to keep contrast low is to maintain variance low (while the vice versa is not true). A low contrast image presents a GLCM concentration term around

the principal diagonal and, consequently, a low value of the GLCM contrast. This result means that high contrast values imply high contrast texture, i.e., first-order statistics contrast and GLCM contrast are strongly related. GLCM contrast and variance were also found to be highly correlated with the first order statistic standard deviation [21], but this condition, according to the theoretical discussion presented above, must be considered as a particular case for the contrast parameter.

D. VARIANCE

$$var = \sum_{i=0}^{N_g-1} \sum_{j=0}^{N_g-1} (i - \mu)^2 \cdot g(i, j) = \overline{\Delta_{var}}$$

Where

$$\Delta_{var} = (i - \mu)^2$$

GLCM variance is a measure of heterogeneity and is strongly correlated to first order statistical variables such as standard deviation [21]. In particular, when a square image area is under textural investigation, the first order statistical variance is equal to the GLCM variance if the GLCM vector displacement is equal to 1 and if its investigation angle is equal to 0° or 90°. Variance increases when the gray level values differ from their mean. Variance is not dependent on the GLCM parameter contrast, in particular when the module of the displacement vector tends to one, since a region may have low spatial frequencies and a low contrast value while its variance may have either a high or a low value (see the theoretical description of the GLCM contrast). Besides, variance requires more computation time than contrast.

E. CORRELATION

$$cor = \sum_{i=0}^{N_g-1} \sum_{j=0}^{N_g-1} (i - \mu) \cdot (j - \mu) \cdot g(i, j) / \sigma^2 = \overline{\Delta_{cor}}$$

Where

$$\Delta_{cor} = (i - \mu) \cdot (j - \mu).$$

GLCM correlation is expressed by the correlation coefficient between two random variables i and j , where i represents the possible outcomes in gray tone measurement for the first element of the displacement vector, while similarly j is associated with gray tones of the second element of the displacement vector. Correlation is a measure of gray tone linear-dependencies in the image [22], in particular, the direction under investigation is the same as vector displacement. High correlation values (close to 1)

imply a linear relationship between the gray levels of pixel pairs.

Thus, GLCM correlation is uncorrelated with GLCM energy and entropy, i.e., to pixel pairs repetitions. Correlation reaches its maximum regardless of pixel pair occurrence, as high correlation can be measured either in low or in high energy situations. GLCM correlation is also uncorrelated to GLCM contrast, as high predictability of the gray level of one pixel from the second one in a pixel pair is completely independent from contrast. As a limiting case of linear-dependency a completely homogeneous area may be considered, for which correlation is equal to 1.

III. SUPPORT VECTOR MACHINE

Pattern recognition by support vector machine (SVM) may be stated as follows: Given a training set (x_i, y_i) (where x_i comprises the input features, $y_i \in \{\pm 1\}$ is the classification output, $i=1, 2, \dots, N$, and N is the number of samples). Optimal margin classification of linearly separable patterns is achieved by finding a hyper plane to separate the two classes $\{+1, -1\}$ on either side of the hyper plane. The decision surface (the hyper plane) is as follows:

$$f(x) = \text{sgn} \left(\sum_{i=1}^N y_i a_i (x_i \cdot x) + b \right)$$

where, the coefficients a_i and b can be determined by solving the large-scale quadratic programming problem:

$$W(\alpha) = \sum_{i=1}^N \alpha_i - \frac{1}{2} \sum_{i,j=1}^N \alpha_i \alpha_j y_i y_j (x_i \cdot x_j)$$

which is subject to the constraints

$$\sum_{i=1}^l \alpha_i y_i = 0, 0 \leq \alpha_i \leq C \text{ for } i = 1, 2, \dots, l$$

The parameter C corresponds to assigning a penalty to tune the tradeoff between minimizing empirical risk (e.g. training errors) and the complexity of the machine. Upon training, only a fraction of the a_i terms are nonzero. For a_i that are nonzero, the corresponding training examples must be nearest to the margins of the decision boundary. These examples are called support vectors.

In most problems, the data are not linearly separable. In order to apply nonlinear transforms to the original data, multiplying all the terms in the feature vector with each other can create a higher dimensional vector. The basic idea is to map the data into another

feature space F where the patterns are linearly separable with a high probability via a nonlinear map $\Phi: R^m \rightarrow F$ and implement the above linear algorithm in F . So, the solution has the form:

$$f(x) = \text{sgn} \left(\sum_{i=1}^N y_i \alpha_i \Phi(x_i) \Phi(x) + b \right)$$

Accordingly, F usually must have very high dimensionality in order to be linearly separable. This can be resolved based on two observations: First, although some mappings have very high dimensionalities, their inner products can be easily computed and second, all the Φ mappings used in the SVM occur in the form of an inner product. So, all the occurrences of inner product resulting from two mappings can be replaced with the kernel function K defined as:

$$K(x, y) = \Phi(x) \cdot \Phi(y)$$

Then, without considering the mapping Φ explicitly, a nonlinear SVM can be constructed by selecting the proper kernel, and the decision function becomes:

$$f(x) = \text{sgn} \left(\sum_{i=1}^N y_i \alpha_i K(x_i, x) + b \right)$$

Polynomial kernel function as one of the three common type kernel functions of SVM is used as:

$$K(x_i, x) = (\gamma x_i^T \cdot x + c)^d, \gamma > 0$$

In this study, $\gamma=1$, $c=1$, and $d=3$.

IV. RESULTS AND DISCUSSION

The performance of the proposed system is evaluated with various test images, where each of them is labeled by radiologist that is liver cirrhosis. The patient database with 40 test samples is separated into two parts: the training database and the test database. These ultrasound images with 430x380 pixels and 256 grays were obtained from B-mode ultrasound imaging system with different tissue harmonic 5.0 and 16 fps.

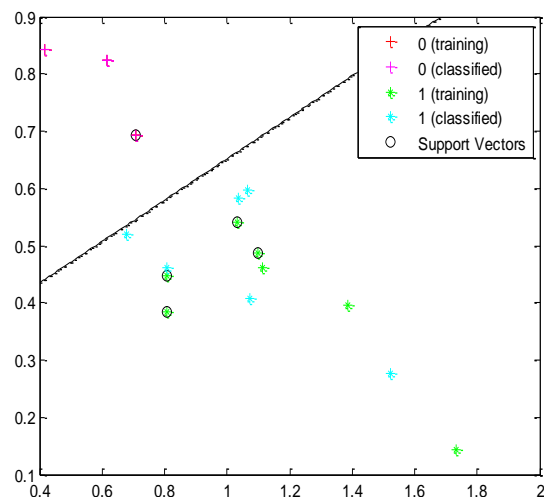


Fig 3: Graph between contrast and correlation of cirrhosis & normal liver

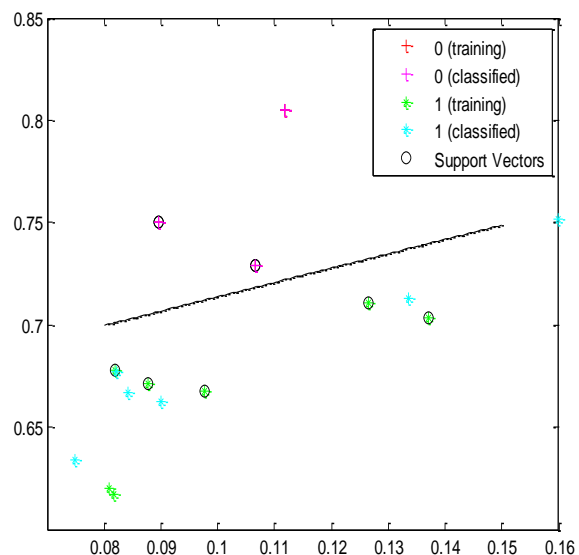


Fig 4: Graph between homogeneity and energy of cirrhosis & normal liver

Fig.3, Fig. 4 & Fig. 5 shows the analysis of the texture parameters of cirrhosis and normal liver that are classified with support vector machine, in which 0 represents normal liver and 1 corresponds to cirrhosis liver. Fig.6 shows an example to detect Regions Of Interest (ROI) from a query image. The detected ROI is much similar with the template in terms of feature difference.

For a fair comparison, we test the performance for both methods under the same condition the ROI is selected manually to answer a query image.

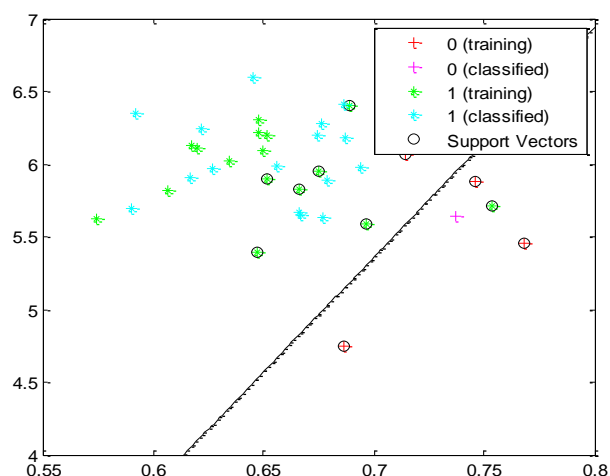


Fig. 5: Graph between homogeneity and entropy of cirrhosis & normal liver

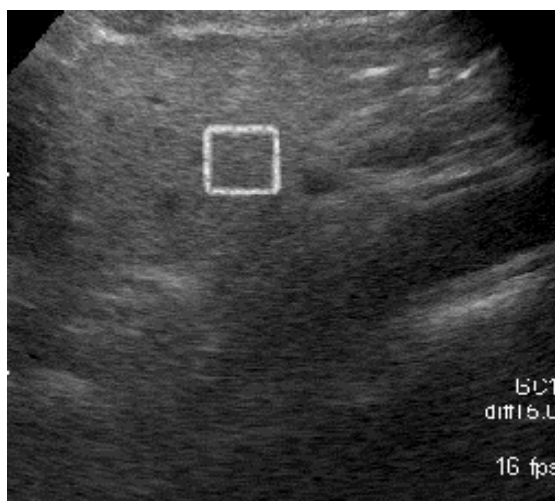


Fig. 6: ROI from an image

Table 1: Classification Accuracy

Classifier	Classification Accuracy
Neural Network Classifier	92.31%
SVM Classifier	94.4%

Table 1 shows the classification accuracy for both methods including neural network and support vector machine for cirrhosis liver detection. In practice, we fix the ROI to the central area of the input query image for classification.

Experimental results show that the proposed method outperforms neural network based approach while diagnosing normal and cirrhosis liver in a system based on ultrasound images.

V. CONCLUSION

In this paper, an image classification method with texture features based on SVM is proposed. The results showed that the support vector machine is 94.4% in sensitivity for liver cirrhosis (LC) while neural network provided 92.31 % in LC. From the experiments results on high- resolution arial images, it has been shown that this method can achieve better results than traditional pixel-based classification method with spectral information used only. The experiment results show that this method is feasible and it can exert the virtues of both spectral and texture features.

REFERENCES

- [1] Vermani, J., Kumar, V., Kalra, N. and Khandelwal, N., "Prediction of Cirrhosis from Liver Ultrasound B-Mode Images based on Laws' Masks Analysis" , *Proc. International Conf. on Image Information Processing*, 2011, 1-5 .
- [2] Bedossa,P., Dargere,D. and Paradis,V., "Sampling variability of liver fibrosis in chronic hepatitis C," *Hepatology*, 38(6), 2003, 1449-1457.
- [3] Nedevschi,S., Vicas, C., Lupsor, M., Badea, R and Grigorescu, M., "The employment of textural and non textural image analysis algorithms in assessing the diffuse liver diseases," *Automat. Comput, Appl. Math.* 17(1), 2008, 12-17.
- [4] Vicas,C., Nedevschi, S., Lupsor, M. and Badea, "Fibrosis detection from ultrasound imaging. The influence of necro-inflammatory activity and steatosis over the detection rates," *Automat. Comput, Appl. Math.*, 16(3), 2007, 26-32.
- [5] Zaid, A., Zaid, S. A. and Fakhr, M. W., "Automatic Diagnosis of Liver Diseases from Ultrasound Images", *Proc. IEEE International Conf. on Computer Engineering and System*, 2006, 313-319.
- [6] Sun, Y.N. and Horng, M.H., "Ultrasonic image analysis for Liver Diagnosis", *Proc. IEEE Conf. on Engineering in Medicine and Biology*, 1996, 93-101
- [7] Takaishi,A., Ogawa, K. and N. &a, "Pattern recognition of diffuse liver diseases by neural networks in ultrasonography," *Proc. of the IEICE (The Institute of Electronics, Information and Communication Engineers) Spring conference*, 1992.
- [8] Ogawa,K. and Fukushima, M., "Computer-aided Diagnostic System for Diffuse Liver Diseases with Ultrasonography by Neural

- Networks,” *IEEE Transactions on Nuclear Science*, 45(6), 1998, 3069-3074.
- [9] Kadah, Y.M., “Statistical and neural classifiers for ultrasound tissue characterization”, *Proc. International conf. on Artificial Neural Networks*, 1993, 1-7.
- [10] Ogawa, K., Hisa, N. and Takaishi, A., “A study for quantitative evaluation of hepatic parenchymal diseases using neural networks in B-mode ultrasonography,” *Med Imag Technol*, 11(1), 1993, 72-79.
- [11] Fukushima, M. and Ogawa, K., “Quantitative Tissue Characterization of Diffuse Liver Diseases from Ultrasound Images by Neural Network”, *IEEE Transactions on Medical Imaging*, 5(2), 1998, 1233-1236.
- [12] Haralick, R.M., Shanmugam, K. and Din, J., “Texture features for image classification, *IEEE Transactions on System, Man and Cybernetics* 1973, 610-621.
- [13] Derya, E. U. and Guler, I., “Feature extraction from Doppler ultrasound signals for automated diagnostic systems”, *Computers in Biology and Medicine*, 35(9), 2005, 735-764.
- [14] Stavroula, G., Mougiakakou and Ioannis, K. V., “Differential diagnosis of CT focal liver lesions using texture features, feature selection and ensemble driven classifiers”, *Artificial Intelligence in Medicine* 41(1), 2007, 25-37.
- [15] Derya, E. U. and Guler, I., “Improving medical diagnostic accuracy of ultrasound Doppler signals by combining neural network models”, *Computers in Biology and Medicine*, 35(7) 2005, 533-554.
- [16] Kadah, Y.M., Farag, A.A., Zurada, M., Badawi, A.M. and Youssef, A.M., “Classification algorithms for quantitative tissue characterization of diffuse liver diseases from ultrasound images”, *IEEE Transactions on Medical Imaging*, 15(4), 1996, 466-477.
- [17] Barber, D.G. and LeDrew, E. F., “SAR sea Ice discrimination using texture statistics: A multivariate approach,” *Photogram Eng. Remote Sensing*, 57(4), 1991, 385-395.
- [18] Gong, P., Marceau, J.D. and Howarth, P.J., “A comparison of spatial feature extraction algorithms for land-use classification with SPOT HRV data,” *Remote Sensing Environ.*, Vol. 40(2), 1992, 137-151.
- [19] Hirose, T.K., McNutt, L. and Paterson, J.S., “A study of textural and tonal information for classifying sea ice SAR imagery,” *Proc. IGARSS '89*, 1989, 747-750.
- [20] Shokr, M.E., “Evaluation of second-order textural parameters for sea ice classification in radar images,” *J. Geophys. Res.*, 96(6), 1991, 10625-10640.
- [21] Dikshit, O., “The classification of texture in remotely sensed environmental imagery,” *Ph.D. dissertation, Univ. Cambridge, Cambridge, UK*, 1992.
- [22] Cossu, R., “Segmentation by means of textural analysis,” *Pixel*, 1(2), 1988, 21-24.
- [23] Qiang, L., Van, M., Wang, N., LIU, Y.H., Wang, S.Q., Wang, L.J., Cheng, J. C., Jin, Y. and Yu, D.Y., “³¹P-MRS Data Analysis of Liver Based on Self-organizing Map Neural Networks”, *Proc. IEEE Asia-Pacific Conf., on Computational Intelligence and Industrial Applications*, 2009, 151-153.